Journal of Proteomics 136 (2016) 234–247

Contents lists available at ScienceDirect

Journal of Proteomics

journal homepage: www.elsevier.com/locate/jprot

In-depth quantitative analysis and comparison of the human hepatocyte and hepatoma cell line HepG2 proteomes

Jacek R. Wiśniewski [a,*], Anna Vildhede [b], Agneta Norén [c], Per Artursson [b,d]

[a] Biochemical Proteomics Group, Department of Proteomics and Signal Transduction, Max Planck Institute of Biochemistry, Martinsried, Germany
[b] Department of Pharmacy, Uppsala University, Uppsala, Sweden
[c] Department of Surgery, Uppsala University, Uppsala, Sweden
[d] Science for Life Laboratory, Uppsala, Sweden

ARTICLE INFO

Article history:
Received 9 September 2015
Received in revised form 28 November 2015
Accepted 25 January 2016
Available online 26 January 2016

Keywords:
Human hepatocyte
Human hepatocyte proteome
Quantitative proteomics
Metabolism
Transporter
ADME proteins
'Proteomic Ruler'
'Total Protein Approach'
FASP

ABSTRACT

Hepatocytes play a pivotal role in human homeostasis. They are essential in regulation of glucose and lipid levels in blood and play a central role in metabolism of amino acids, lipids, drugs and xenobiotic-compounds. In addition, hepatocytes produce a major portion of proteins circulating in the blood. Hepatocytes were isolated from liver tissue obtained from surgical resections. Proteins were extracted and processed using filter aided sample preparation protocol and were analyzed by LC–MS/MS using high accuracy mass spectrometry. Proteins were quantified by the 'Total Protein Approach' and 'Proteomic Ruler'. We report a comprehensive proteomic analysis of purified human hepatocytes and the human hepatoma cell line HepG2. The complete dataset comprises 9400 proteins and provides a comprehensive and quantitative depiction of the proteomes of hepatocytes and HepG2 cells at the protein titer and copy number dimensions. We describe basic cell organization and in detail energy metabolism pathways and metabolite transport. We provide quantitative insights into protein synthesis and drug and xenobiotics catabolism. Our data delineate differences between the native human hepatocytes and HepG2 cells by providing for the first time quantitative data at protein concentrations and copy numbers.

1. Introduction

The human liver is the largest internal organ of the human body constituting 2.5% of an adult's body weight. It plays an important role in maintaining glucose levels and regulating lipid titers in the blood. The liver is a key organ for the metabolism of drugs and other xenobiotic compounds. It also plays a central role in lipid and amino acid metabolism. Many of the proteins circulating in the blood, such as albumin constituting 55–70% of the total protein in plasma, are produced in the liver. The liver functions as an excretory organ for bile and cholesterol. It carries out endocrine functions by modifying or amplifying hormone action and degrading circulating hormones. Finally, the liver is an important storage organ for glycogen, fat-soluble vitamins, and iron.

The liver is composed of several types of highly specialized cells: hepatocytes, Kupffer, stellate, and sinusoidal endothelial cells. The hepatocytes are the major fraction of cells representing about 80% of the liver cell population. They are nearly cubical cells with 15 μm sides [1] and have relatively small nuclei occupying 5–7% of the cell volume [2]. Hepatocytes are often binucleated and their nuclei are frequently anisokaryotic. The hepatocytes are rich in endoplasmic reticulum and mitochondria reflecting their intense protein synthesis and energy metabolism, respectively. Because of their pivotal role in human homeostasis, hepatocytes have been subject of numerous studies capturing their morphology and biochemistry [3]. Additionally, hepatocytes have been raising a particular attention to pharmacologists investigating the uptake, metabolism, excretion, and toxicity of drugs [4]. Due to the limited availability of fresh human hepatocytes, hepatoma cell lines, such as HepG2 cells, are frequently used as in vitro substitutes [5,6].

Whereas classical biochemical approaches allow analysis of only a limited number of proteins or enzymes, deep-proteome analyses have the potential to cover thousands of proteins analyzing minute amounts of biological material [7,8]. In this type of proteomic analysis the measured spectral intensities of peptides of the digested proteins can be transformed into protein concentrations and protein copies per cell using the 'Total Protein Approach' [9] and the 'Proteomic Ruler' computational method [10], respectively. Recently, we have applied this technology to analyze titers of drug transporters and other

* Corresponding author at: Biochemical Proteomics Group, Department of Proteomics and Signal Transduction, Max-Planck-Institute of Biochemistry, Am Klopferspitz 18, D-82152 Martinsried, Germany.
E-mail address: jwisniew@biochem.mpg.de (J.R. Wiśniewski).

http://dx.doi.org/10.1016/j.jprot.2016.01.016

proteins involved in the biotransformation of drugs and xenobiotic compounds in membrane fractions isolated from human liver and hepatocytes [11–13]. In addition, we used our technology to establish quantitative proteomic maps of a variety of mouse tissues including small intestine [14], liver [15] and skeletal muscle [16]. In this study we performed an in-depth proteomic analysis of purified human hepatocytes and the hepatoma cell line HepG2. Our dataset encompass 9400 proteins providing a comprehensive and quantitative repository of proteins. Our data delineate the subcellular architecture and organization of metabolic pathways and demonstrate differences between hepatocytes and the cultured HepG2 cells. We report the first in-depth and quantitative analysis of the hepatocyte proteome.

2. Materials & methods

2.1. Human hepatocytes

Samples of normal human liver tissue were obtained from 7 donors undergoing surgical resections carried out at the Department of Surgery at Uppsala University Hospital. All donors gave their informed consent. Ethical approval was granted by the Uppsala Regional Ethics Committee (ethical approval no 2009/028). Clinical characteristics of the patients are given in Supplemental Table 1. Hepatocytes were isolated by the two-step collagenase isolation procedure [17] and stored at −80 °C until subcellular fractionation and proteomic analysis.

2.2. Cell culture

The human hepatoma cells HepG2 (ATCC HB-8065) were grown in Eagle's Minimum Essential Medium supplemented with 10% fetal calf serum and 1% streptomycin. The cells were harvested at 70% confluence and stored at −80 °C until proteomic analysis.

2.3. Subcellular fractionation of hepatocytes

The frozen hepatocytes were thawed on ice and suspended in homogenization buffer composed of 0.3 M sucrose, 10 mM $MgCl_2$, and 50 mM Tris–HCl, pH 7.8. The cells were homogenized at 0 °C in a Teflon-Glass Potter S homogenizer at 1200 rpm with 10 down-up cycles. The crude nuclear fraction was obtained by centrifugation of the homogenate at 1000 ×*g* for 10 min. The post-nuclear supernatant was used for isolation of membrane fractions and cytosol. The crude nuclear pellet was suspended in the HB buffer and the suspension was layered onto a 'sucrose cushion' consisting of 2 M sucrose. After centrifugation at 16,000 ×*g* for 20 min the supernatant was discarded and the pellet containing purified nuclei was washed twice with the HB buffer. The post-nuclear supernatant was centrifuged at 200,000 ×*g* for 40 min. The resulting supernatant was designated as 'cytosol' whereas the pellet was extracted with 0.1 M Na_2C0_3 and 5 M urea to purify the membrane fractions as described previously [18].

2.4. Sample preparation

The hepatocytes, hepatocyte subcellular fractions, and cultured HepG2 cells were lysed in 0.1 M Tris–HCl, pH 7.6, containing 50 mM DTT and 2% SDS (*w*/*v*) in boiling water bath for 4 min. After cooling to room temperature the lysates were clarified by centrifugation at 16,000 ×*g* for 10 min. The lysates were processed according to the MED-FASP protocol using endoproteinase LysC and trypsin [19]. Total protein and total peptide contents were determined using a tryptophan-fluorescence assay [20]. Peptides were fractionated using pipette tip SAX as described previously [21] The LysC-peptides from whole cell lysates (samples A–G) were fractionated into 4 fractions eluting at pH 12, 6, 4, and 2 whereas the tryptic peptides were eluted at pH 5 and 2. The LysC and tryptic peptides from subcellular fractions (samples D and E) were eluted at pH 5 and 2. Except for fractions D and E the analyses were performed in duplicates. Two samples (F and G) were also processed by PEGylation strategy into two LysC and two tryptic fractions of Cys-depleted peptides and one Cys-enriched peptide fraction [22].

2.5. Mass spectrometry and data analysis

Aliquots of peptides were separated on a reverse phase column and analyzed on a QExactive mass spectrometer (Thermo) as described previously [7]. Briefly, the peptides were separated on a reverse phase column (20 cm × 75 μm inner diameter) packed with 1.8 μm C18 particles (Dr. Maisch GmbH, Ammerbuch-Entringen, Germany) using a 4 h acetonitrile gradient in 0.1% formic acid at a flow rate of 250 nl/min. The liquid chromatography was coupled to a QExactive mass spectrometer (Thermo Fisher Scientific, Germany) via a nanoelectrospray source (Proxeon Biosystems, now Thermo Fisher Scientific). The QExactive was operated in data-dependent mode with survey scans acquired at a resolution of 50,000 at m/z 400 (transient time 256 ms). Up to the top 10 most abundant isotope patterns with charge ≥ +2 from the survey scan were selected with an isolation window of 1.6 Th and fragmented by HCD with normalized collision energies of 25. The maximum ion injection times for the survey scan and the MS/MS scans were 20 ms and 60 ms, respectively. The ion target value for both scan modes were set to 10^6. The dynamic exclusion was 25 s and 10 ppm.

2.6. Data analysis

The raw data were analyzed with MaxQuant Software (Ver. 1.2.6.20) using the human UniProt database (Vers. May 2013). The search was performed with a fragment ion mass tolerance of 0.5 Da and parent ion tolerance of 20 ppm. The protein and peptide false discovery rates were set to 1%. Protein abundances were calculated from the spectral raw intensities using the 'Total Protein Approach' [9,23] using the relationships:

$$\text{Total protein (i)} = \frac{\text{MS} - \text{signal (i)}}{\text{Total MS} - \text{signal}}$$

or

$$\text{Protein concentration (i)} = \frac{\text{MS} - \text{signal (i)}}{\text{Total MS} - \text{signal} \times \text{MW(i)}} \left[\frac{\text{mol}}{\text{g total protein}}\right].$$

The total protein content of the cells and the protein copy number per cells was assessed using the 'Proteomic Ruler' approach assuming a DNA content of human cells of 6.5 pg [10] using the relationship:

$$\text{Total protein/nucleus} = \frac{6.5\ \text{pg} \times \text{Total MS} - \text{signal}}{\text{MS} - \text{signal (Total histone)}}\ [\text{pg}];$$

and

$$\text{Protein copy number} = N_A \times \text{Total protein/nucleus} \times \text{Protein concentration},$$

where N_A is the Avogadro number. The calculations were performed in Microsoft Excel (Supplemental Table 2, sheet 'Histone ruler').

2.7. Statistical analysis

Protein concentration and copy number data were processed using Perseus software 1.5.0.8 (http://www.perseus-framework.org/). For

the calculation of significances of protein abundance differences between hepatocytes (7 values) and HepG2 cells (3 values) the minimal number of values was set to 7 per protein. 6129 proteins passed this filter. Imputation of missing values occurred through generation of random numbers that are drawn from a normal distribution. The parameters of this distribution can be optimized to simulate a typical abundance region that the missing values would have if they had been measured. We used the parameter values of 0.3 for width and 1.8 for down shift. Typically the missing values simulate low abundance measurements. The t-test significances were calculated using the threshold of 0.05 FDR (Supplemental Table 3).

3. Results & discussion

3.1. Experimental design and sample analysis

Hepatocytes isolated from livers of 7 donors were used in this study. On the basis of the abundance of cell-specific marker proteins in the hepatocyte fractions compared to whole liver the hepatocytes were well depleted from Kupffer and stellate cells and were enriched at least 10-fold in respect to sinusoidal endothelial cells (Fig. 1A). To obtain a global picture of the hepatocyte proteome, whole cell lysates were analyzed. This resulted in an identification of 8705 proteins, of which

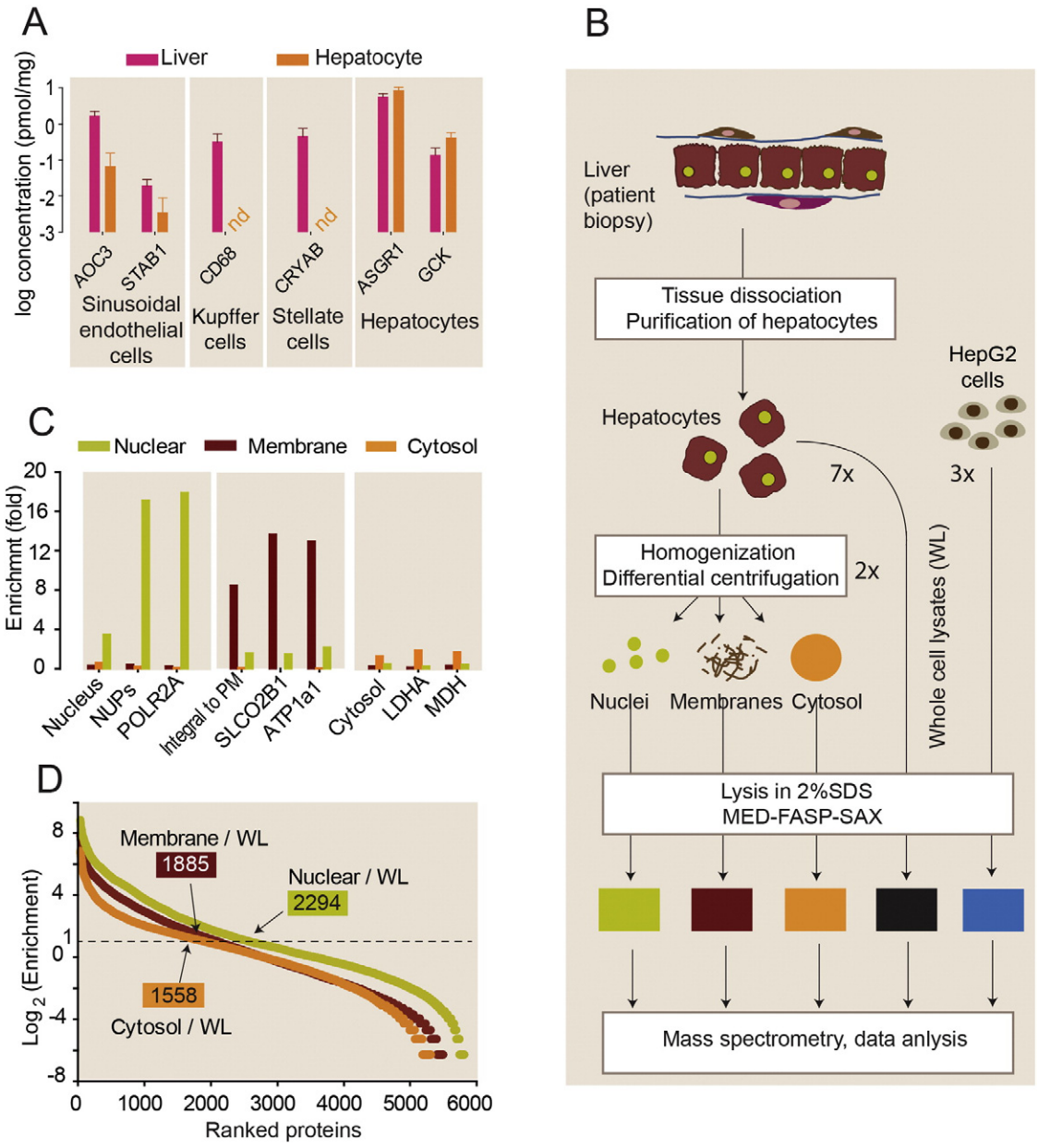

Fig. 1. Quantitative proteomic analysis of the human hepatocyte proteome. (A) Purity of the hepatocyte preparations. Proteins specific for other liver cell types than hepatocytes were depleted. The titers of the marker proteins in human liver are from [11]. (B) Workflow of the analysis. Hepatocytes were either lysed in SDS-containing buffer or were homogenized and fractionated into nuclear, membrane and cytosolic fractions before the lysis. The lysates were processed by MED-FASP and the resulting peptides were fractionated on SAX columns and analyzed by LC–MS/MS. The mass spectra were processed by the MaxQuant software and the raw spectral intensities were used for calculation of protein abundances using the TPA method [23]. (C) Enrichment of marker proteins in the subcellular fractions. The enrichment values were calculated as the ratio of the protein concentration in the fractions to that in whole cell lysate. 'Nucleus', 'Integral to plasma membrane', and 'Cytosol' refer to average values calculated from abundances of all proteins matching these GO categories. (D) Subcellular fractionation allows discrimination between proteins associated with cell membranes, nuclei and cytosol.

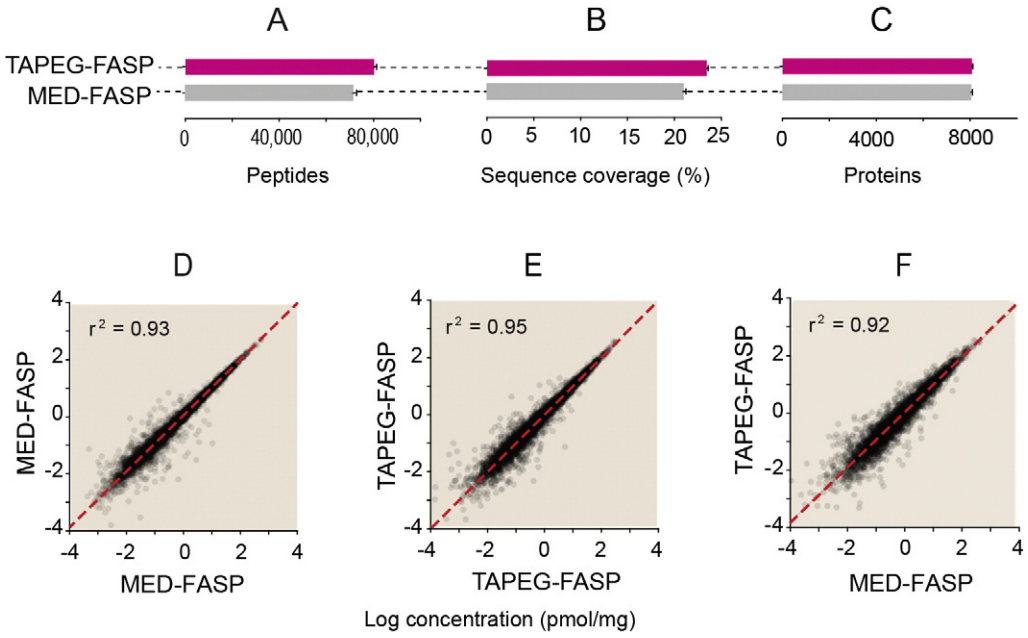

Fig. 2. Comparison of MED FASP and TAPEG FASP for analysis of whole lysates of human hepatocytes. (A) Number of identified peptides per sample. (B) Protein sequence coverage. (C) Number of identified proteins per sample. Run-to run reproducibility using concentrations of proteins identified with more than 2 peptides: MED-FASP vs. MED-FASP (D), TAPEG FASP vs. TAPEG FASP (E) and MED-FASP vs. TAPEG-FASP (F).

97% were matched with at least two peptides (Supplemental Table 2). Additionally, to provide insights into the subcellular location of proteins two of the hepatocyte samples were further separated into nuclear, post-nuclear membrane and cytosolic fractions. (Fig. 1B). These analyses extended the hepatocyte proteome by 337 additional proteins. Moreover, to increase the depth of proteomic analysis of lysates from the hepatocyte samples F and G were also processed with TAPEG-FASP method [22]. In this approach SH-reduced proteins are modified with thiol-activated polyethylene glycol (TAPEG) before consecutive protein digestion with LysC and trypsin and isolation of two fractions of non-derivatized peptides. After reduction of disulfide bonds between cysteine containing peptides and the polyethylene glycol moieties, a third fraction of peptides is collected. Comparison of the results showed that TAPEG-FASP enable identification of more peptides than MED-FASP (Fig. 2A). This results in an average increase of protein sequence coverage by 10% (Fig. 2B), but has little effect on the number of identified hepatocyte proteins (Fig. 2C). This result resembles the outcome of the analysis of mouse liver [22]. In terms of run-to run reproducibility of MED-FASP and TAPEG-FASP were comparable (Fig. 2D-F). Notably, similar reproducibility was reported for other sample fractionation approaches [24]. Furthermore, an analysis of 3 samples of HepG2 cells extended the dataset by 313 proteins, which were specific to these cells (Supplemental Table 2).

Comparison of the protein concentrations in the nuclear, membrane and cytosolic fractions with those in whole lysates allowed for calculation of enrichment values for each of the subcellular components (Fig. 1C). Based on the abundances of polypeptides involved in organization of nuclear pores (NUPs) and the RNA polymerase II, the enrichment of nuclear proteins was about 17-fold. This value is close to the theoretically possible enrichment of 14- to 20-fold assuming that the nuclei constitute 5–7% of the total cell protein. Similarly, high enrichment values of 13–14-fold were found for the plasma membrane proteins organic anion transporting polypeptide (OATP) 2B1 (*SLCO2B1*) and the α-subunit of the Na^+/K^+-pump (*ATP1A1*) (Fig. 1C). The enrichment of the cytosolic proteins lactate and malate dehydrogenases in the cytosolic fraction was about 2-fold, reflecting that this fractions constitute about 50% of the cell. The isolation of the subcellular fractions of the hepatocytes resulted in the identification of 1558 cytosolic, 1885 membrane, and 2294 nuclear proteins that were enriched at least 2-fold compared to the whole lysate (Fig. 1D).

3.2. Statistical analysis of the differences between the hepatocyte and HepG2 cell proteomes

At total of 6129 proteins were identified in at least 7 out of the 10 in total whole lysate samples of the hepatocytes and HepG2 cells. These were subjected to calculation of protein ratios and subsequent statistical analysis. Principal component analysis of the protein concentrations as well as protein copy numbers revealed a clear separation of the hepatocyte and HepG2 samples (Fig. 3A and B). T-test analysis allowed determination of the statistical significance of the protein differences. In total, concentrations of 4857 proteins and copy numbers of 3936 proteins were significantly (FDR < 0.05) upregulated of downregulated for the hepatocytes and HepG2 line (Fig. 3C and Supplemental Table 3). 3191 significant changes were common to both analyses. 1665 significant changes were unique to the concentration values, whereas 745 were specific to copy numbers. This difference clearly shows that proteomic comparisons of cells that are different in their sizes should be performed with a particular care. The proportion of proteins organized in specific organelles should be considered. Fig. 3D shows that the number of significantly changed proteins in relation to their cellular location varies between the two different calculation methods. Compared to the analysis of differences in protein concentrations, the analysis of protein changes in copy numbers decreases the number of significant hits for nuclear and nucleolar proteins by about 40%. The opposite happens with the numbers of significant changes related to plasma membrane and mitochondrial proteins, which frequency increases by 10 and 30% respectively. These differences reflect distinct contribution of different organelles to the total protein of the cell.

The large extent of significant differences for the hepatocytes and HepG2 cells reflects both structural and physiological dissimilarities for these biological systems. Previously we observed a similar degree of differences between white and red muscle fibers [26] and between human colon mucosa and its adenoma and cancer [27].

We are also aware that some differences in protein titers could be related to the various ages of the liver donors. Whereas the hepatocytes

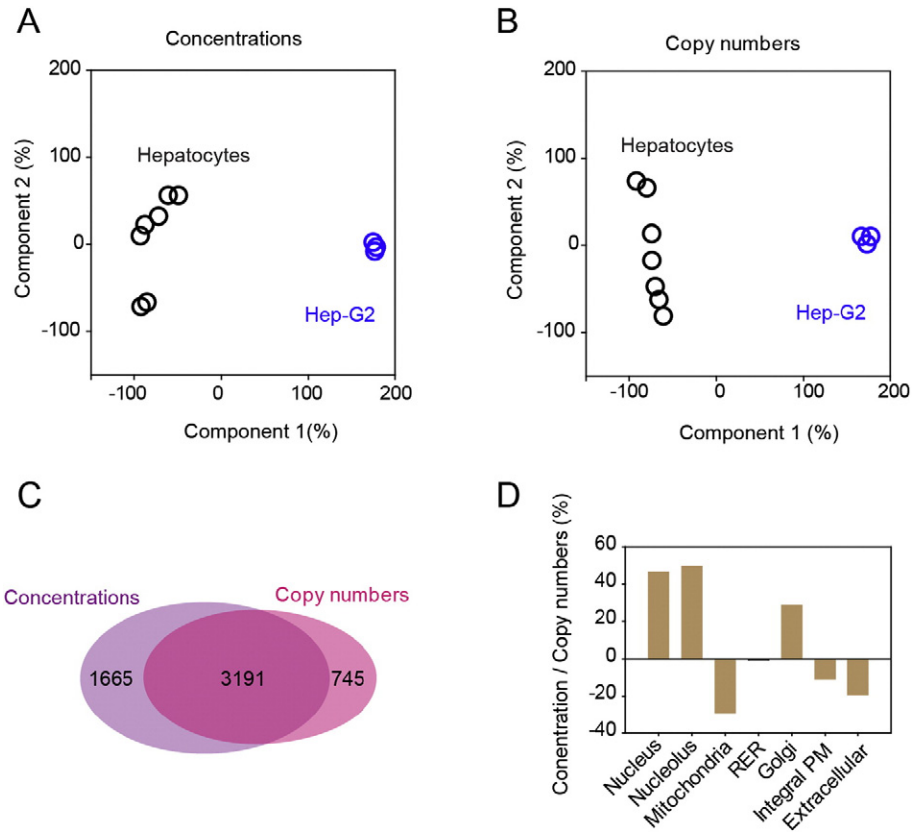

Fig. 3. Statistical analysis. (A) and (B) Principal component analyses of the concentration and copy number values. (C) Overlap between significantly changed proteins assessed from concentration and copy number data. (D) Comparison of the cellular location (GO terms) of the non-overlapping significantly changed proteins. The values were calculated using the formula: {(number of proteins with significantly changed concentration / number of proteins with significantly changed copy number)−1} × 100%.

were isolated from donors, which were older than 60 years, the HepG2 cells originate from a 15 year male. Age related changes in liver include increases size and ploidy of hepatocytes and altered liver metabolism and secretion are well documented [28].

3.3. Overview of the human hepatocyte and HepG2 cell proteomes

The human hepatocyte is described by a number of morphometric and biochemical studies. These analyses provide detailed measures of the volume, protein content, and subcellular composition as well as quantitative information on abundance and activity of specific proteins. Recently, we have proposed delineation of cell composition by combining protein abundances measured using the TPA method and cell compartment annotations given by 'Gene Ontology' [9]. We have shown that this kind of analysis allows detection of alterations in the architecture of cells undergoing a neoplastic transformation or differentiation [9] or those exposed to a physiological stress [14]. In addition, this approach is useful to study protein composition of organelles such as mitochondria [15]. Applying the 'Histone ruler' concept, total protein contents calculated by TPA can be converted into protein copies per cell and for organelle-specific proteins into copies per organelle type. Using these computational tools, we have calculated the protein content per single nucleus and the content of the basic subcellular components of the hepatocyte and the HepG2 cell (Fig. 4A-C). Due to the fact that about 20% of human hepatocytes are binucleated or polyploid [29], the copy number values per cell are about 1.2-fold higher compared to those per nucleus containing 2n DNA. However, these numbers vary between donors as a result of factors such as age or disease [29,30].

The modal number of chromosomes in the HepG2 cells is 55, while the corresponding number in somatic human cells is 46. We previously determined DNA content in the HepG2 cells and found 7.5 pg DNA per cell [10]. This is only 15% more compared to the normal somatic cell. Therefore the copy number values in HepG2 could be up to 15% higher, resembling the situation in the hepatocytes. For this reason we did not correct the protein copy numbers.

The 'Proteomic Ruler' revealed that human hepatocytes contained on average 600 pg total protein per cell. In contrast, HepG2 cells were smaller with on average 170 pg of total protein per cell. Since the total concentration of proteins in eukaryotic cells lies within a range of 200 to 300 g/l [31], the hepatocyte and HepG2 cell were determined to have volumes of 3000 μm^3 and 850 μm^3, respectively (Fig. 4A). The calculated hepatocyte volume is close to a textbook value of 3400 μm^3 [1].

Analysis of the subcellular composition of the hepatocyte revealed that the mitochondria made up about 25% of the total cellular protein whereas the endoplasmic reticulum (ER) and Golgi apparatus together constituted 12% of the total protein (Fig. 4B). The nuclei of the hepatocytes constituted on average 10% of the total protein. These values are similar to the data obtained in a morphometric study of the mononuclear rat hepatocytes, estimating the cellular content of nucleus, ER and mitochondria to 6, 16, and 23%, respectively [2].

Compared to the hepatocytes, abundances of the organelles in HepG2 cells were quite different (Fig. 4B). The nuclei of the HepG2 cells constituted as much as 25% of the total cellular protein whereas mitochondria contained only 12% of the total protein. Because HepG2 cells are about 3 times smaller than the hepatocytes, the sizes of the nuclei in both cell types were similar, containing 7–9 × 10^8 protein molecules (Fig. 4C). This may indicate that the apparatus of maintaining and processing genetic information is of a similar size in both cell types. In contrast, organelles primarily involved in protein synthesis and protein maturation, i.e., ER and Golgi, as well as energy production, mitochondria, contained on average one order of magnitude more molecules in human hepatocytes compared to HepG2 cells. Proteins integral to the

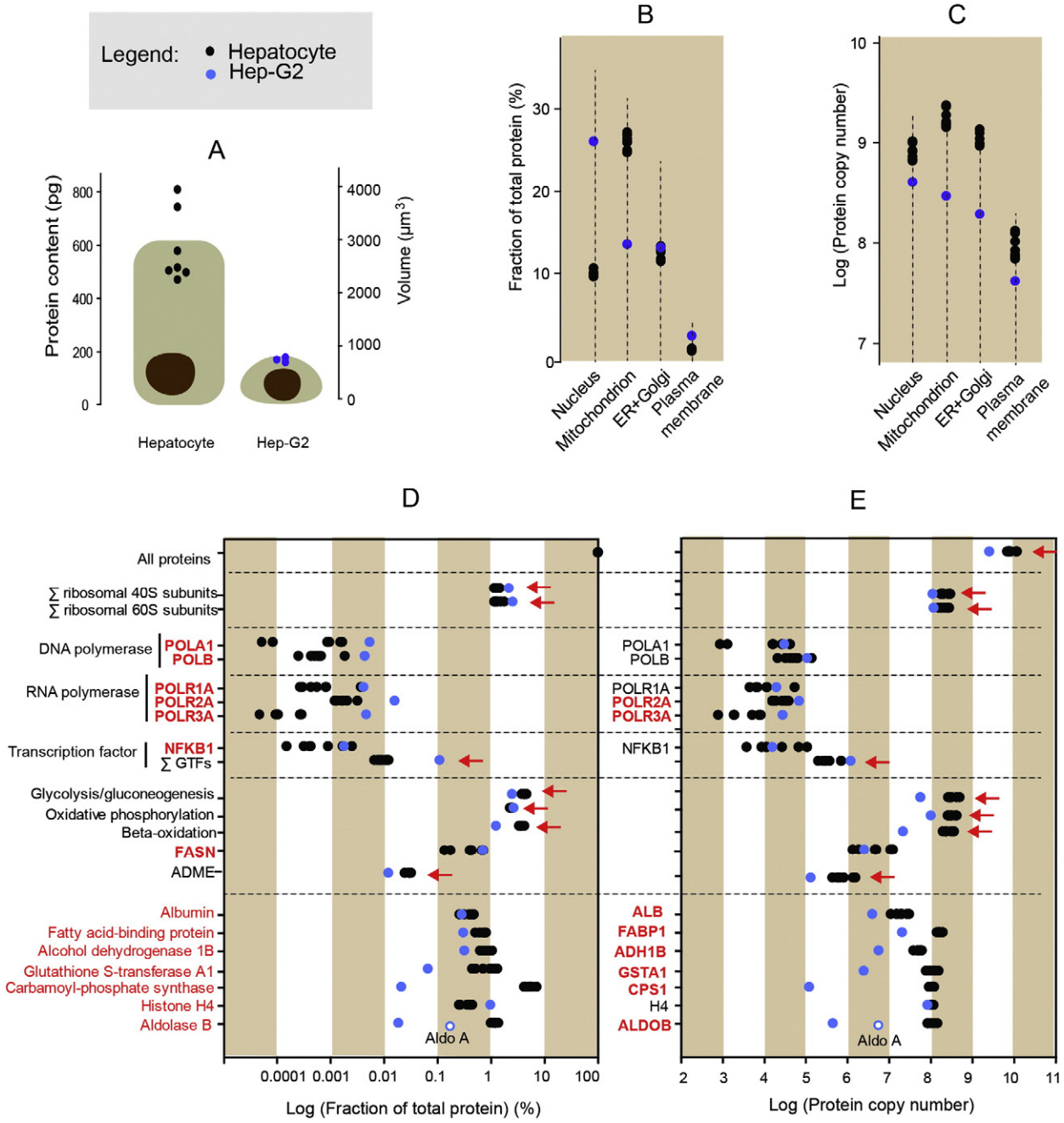

Fig. 4. Basic elements of the human hepatocyte proteome. (A) Total protein content and cell volume per nucleus of the hepatocytes and the cultured HepG2 cells calculated using the 'Proteomic Ruler' [10]. The cell volume was calculated using the assumption of an average cellular protein concentration of 20%. (B and C) Protein content of selected organelles and their membrane fractions expressed as fraction of the total protein (B) or cumulative copy number (C). (D and E) Examples of the content of selected cellular assemblages, pathways, and the most abundant proteins of the hepatocytes. Black and blue dots, show average abundance values calculated for the 7 hepatocyte and 3 HepG2 cell samples, respectively. Gene names of proteins with statistically significant titer-differences between hepatocyte and HepG2 are in red (FDR < 0.05). Arrows indicate statistically significant abundance-differences between HepG2 and hepatocytes at the selected protein groups ($P < 0.001$). The x-axis label in E shows exponents only.

plasma membrane constituted about 1.2% of the total protein in hepatocytes (Fig. 4B) whereas HepG2 cells harbored two times more of these proteins. However, when the abundances of plasma membrane proteins were expressed in copies per cell, hepatocytes contained more of these proteins compared to HepG2 cells (Fig. 4C). This presumably reflects a several-fold larger cell surface of a hepatocyte compared to a HepG2 cell.

The human hepatocyte was found to be composed of on average 8.7×10^9 protein molecules whereas a HepG2 cell only contained 2.5×10^9 (Fig. 4E). Ribosomal proteins of the large and small subunits constituted each 1.3% of total protein in human hepatocytes and about 2.3% in HepG2 cells (Fig. 4D). However, in copy number terms, human hepatocytes contained on average 2 times more ribosomal proteins than HepG2 cells (Fig. 4E). The copy numbers for the RNA polymerase 1 and general transcription factors were similar for the hepatocytes and HepG2 cells whereas RNA polymerases 2 and 3 were 2.6 and 7.2-fold more abundant in the HepG2 cells (Fig. 4E). Copy numbers of proteins directly involved in DNA replication, such as the DNA polymerase subunits (POLA-POLE), minichromosome maintenance helicase complex subunits MCM2-MCM7, replication factor c (RFC1-RCF5), proliferating cell nuclear antigen and (PCNA) and the Ribonuclease H (RNASEH2C) were 2.5–20 fold higher in the HepG2 cells compared to

the hepatocytes (Fig. 4E, and Supplemental Table 2). Out of these 19 proteins, 15 showed statistically significant differences in copy numbers (Supplemental Table 3). These differences obviously reflect lower replication and cell division rate of the hepatocytes compared to the cultured cells.

Glycolysis/gluconeogenesis, β-oxidation of fatty acids and oxidative phosphorylation were the most abundant metabolic pathways in the hepatocytes. Each involved 1–5 × 10^8 protein molecules (Fig. 4E) and constituted 2–3% the total protein (Fig. 4D). Recently, we have reported similar abundances in mouse liver [15]. For comparison, the major components of the fatty acid synthesis system constituted about 10 times less total protein in the HepG2 cells and the whole set of proteins involved in drug biotransformation (see below) accounted for 1000,000 molecules in the human hepatocyte but only 100,000 molecules in the HepG2 cell.

Next, we compared the abundances of single proteins (Fig. 4D and E). In the hepatocytes, fatty acid binding protein (all isoforms together) was the most abundant in respect to its number of copies while carbamoyl phosphate synthase (CPS) was the most abundant by mass (4–6% of total mass) (Fig. 4D). Considering that mitochondria occupy 25% of the hepatocyte, CPS constituted 20% of total mitochondrial protein. We have recently reported a comparable value for mouse liver [15]. Serum albumin, being synthesized by hepatocytes, was another highly abundant protein. It constituted on average 2 × 10^7 copies per cell which accounted for 0.3% of the total protein of the hepatocyte. In the HepG2 cells, the titers of albumin and CPS were about one order of magnitude lower than in the hepatocytes. The differences between the HepG2 cell line and native hepatocytes were not only restricted to titers of proteins but also manifested itself in changes from one isoform to another. For example, aldolase B was the key enzyme in hepatocytes whereas the dominant isoform in the HepG2 cells was aldolase A, which is most common in normal muscle tissue (Fig. 4D and E).

3.4. Protein synthesis

Hepatocytes are responsible for synthesis of many extracellular proteins. The most prominent are serum albumin, clotting factors, and α- and β-globulins. These proteins play vital roles in the organism and can often be used as markers for liver diseases. Protein synthesis starts with ligation of amino acids to their specific transfer RNAs (tRNAs) and often ends with attachment of sugar moieties (Fig. 4).

Ligation of the amino acids to their respective tRNA is the first step in the assembly of proteins. We found a correlation between the concentrations of the amino acid tRNA synthases and the frequency of the amino acids in the hepatocyte proteome (Fig. 5A). The Cys-tRNA and Trp-tRNA synthases showed the lowest concentrations of about 1 pmol/mg, which reflects the lowest frequency of cysteine and tryptophan in the hepatocyte proteome. In contrast, the summed abundance of Leu-tRNA and Ile-tRNA synthases was high (about 5 pmol/mg) and related to the highest frequency of these amino acids. In respect to the amino acid frequency, tRNA synthases of aspartic acid and tyrosine appeared to be more abundant compared to other tRNA synthases. In the HepG2 cells, the titers of the amino acid tRNA synthases were on average 2-fold higher than in the hepatocytes. This obviously reflects higher titers of the RNA polymerase 2 in HepG2 cells compared to the hepatocytes (Fig. 4D). Notably, titers of the major factors involved in elongation were also about two times more abundant in the HepG2 cells than in the hepatocytes (Fig. 5B). The higher abundances likely reflect differences in cell division. The HepG2 population doubles about every 24 h, while primary hepatocytes of adult livers divide only rarely.

Protein glycosylation is a common posttranslational modification of the extracellular proteins. Generally, this modification falls into one of two classes, the N-type at the asparagine residues and the O-type at serine residues [32,33]. Both types of glycosylation involve complex machineries synthesizing and attaching glycan moieties to proteins. In the case of the N-glycosylation a series of reactions leads to the formation of a glycan precursor, the dolichol-P–P-$GlcNAc_2Man_9Glc_3$ and its attachment to asparagine residues by the oligosaccharyltransferase complex (OST) [33]. Both the dolichol-P–P-$GlcNAc_2Man_9Glc_3$ and the OST complex had higher titers in the hepG2 cells compared to the hepatocytes (Fig. 5C). In contrast, titers of enzymes involved in O-glycosylation varied for the two types of cells (Fig. 5D). Whereas titers of sialylating and fucosylating transferases were higher in hepatocytes than in HepG2 cells, titers of transferases of UDP-glucose and xylose and UDP-N-acetylglucosamine were higher in HepG2 cells. The deficiency in salylated glycans is common to cultured cell lines [34].

The liver is the main source of plasma proteins. In Fig. 5E we compared the cellular concentration of several prominent plasma proteins with their concentrations in plasma [15]. We observed that the concentrations of plasma proteins in the hepatocytes were similar or higher compared to their titers in plasma. In HepG2 cells, titers of serum albumin, transferrin and SERPINA1 were similar to those in human hepatocytes, whereas other proteins, including ceruloplasmin (*CP*), were down-regulated. Hemopexin (*HPX*), which transports heme into the liver for breakdown and iron recovery, was not detected in the HepG2 cells.

3.5. Energy metabolism

Energy metabolism consists of diverse cellular processes dedicated to energy supply and storage. The major pathways involved in these processes are shown in Fig. 6.

Glucose, after phosphorylation by hexokinase or glucokinase to G6P, can be directly used for production of ATP through glycolysis, converted into glycogen, or can enter the pentose phosphate pathway allowing the redirection of metabolic fluxes to meet a variety of physiological requirements (Fig. 6 **A–C**). The latter pathway plays a key role in providing NADPH for lipid synthesis and pentose precursors for synthesis of nucleic acids. Furthermore, via the gluconeogenic process, which also involves some glycolytic enzymes, G6P can be produced from pyruvate. We observed clear differences between hepatocytes and HepG2 cells with regards to energy metabolism pathways. For example, 1,6-glucose bisphosphatase (*FBP1*), the key enzyme of the gluconeogenesis, was 3 orders of magnitude less abundant in HepG2 cells than in hepatocytes (Fig. 6A). Notably, this enzyme was the most abundant of the key metabolic enzymes in hepatocytes with titers of over 100 pmol/mg (Fig. 6A). The high abundance of FPB together with high titers of lactate dehydrogenase points at the role of liver in the Cori cycle in which the hepatocytes convert lactate released from muscles to glucose.

Glycogen is the key energy storage depot in hepatocytes. The titers of enzymes involved in the synthesis and degradation of glycogen were 1–2 orders of magnitude higher in the hepatocytes compared to the HepG2 cells (Fig. 6B), indicating that in the latter the glycogen metabolism is negligible.

Pyruvate, the final product of the glycolysis, undergoes decarboxylation to acetyl-CoA by pyruvate dehydrogenase. This enzyme is composed of multiple copies of three major subunits: PDH (including isoforms A, B and X), DLAT, and DLD (Fig. 6D). The concentrations of these proteins in the hepatocytes and the HepG2 cells were within 1-10 pmol/mg. Similar concentrations of the pyruvate dehydrogenase components are found in whole mouse liver lysates [15]. Acetyl-CoA may be used in the Krebs cycle to produce energy equivalents, NADH. Similarly to the enzymes involved in the glycolysis, the titers of many Krebs cycle enzymes varied between the hepatocytes and the HepG2 cells. For example, in HepG2 the concentration of citrate synthase was 5 times higher than in the hepatocytes (Fig. 6E).

Moreover, the abundances of the iso-citrate dehydrogenases 2 and 3 showed clear differences between the native and cultured cells. In the hepatocytes, the dehydrogenation of iso-citrate appeared to be carried out mainly by IDH2 which releases NADPH, whereas IDH3 (3 subunits), producing NADH, was the more abundant enzyme in the cultured

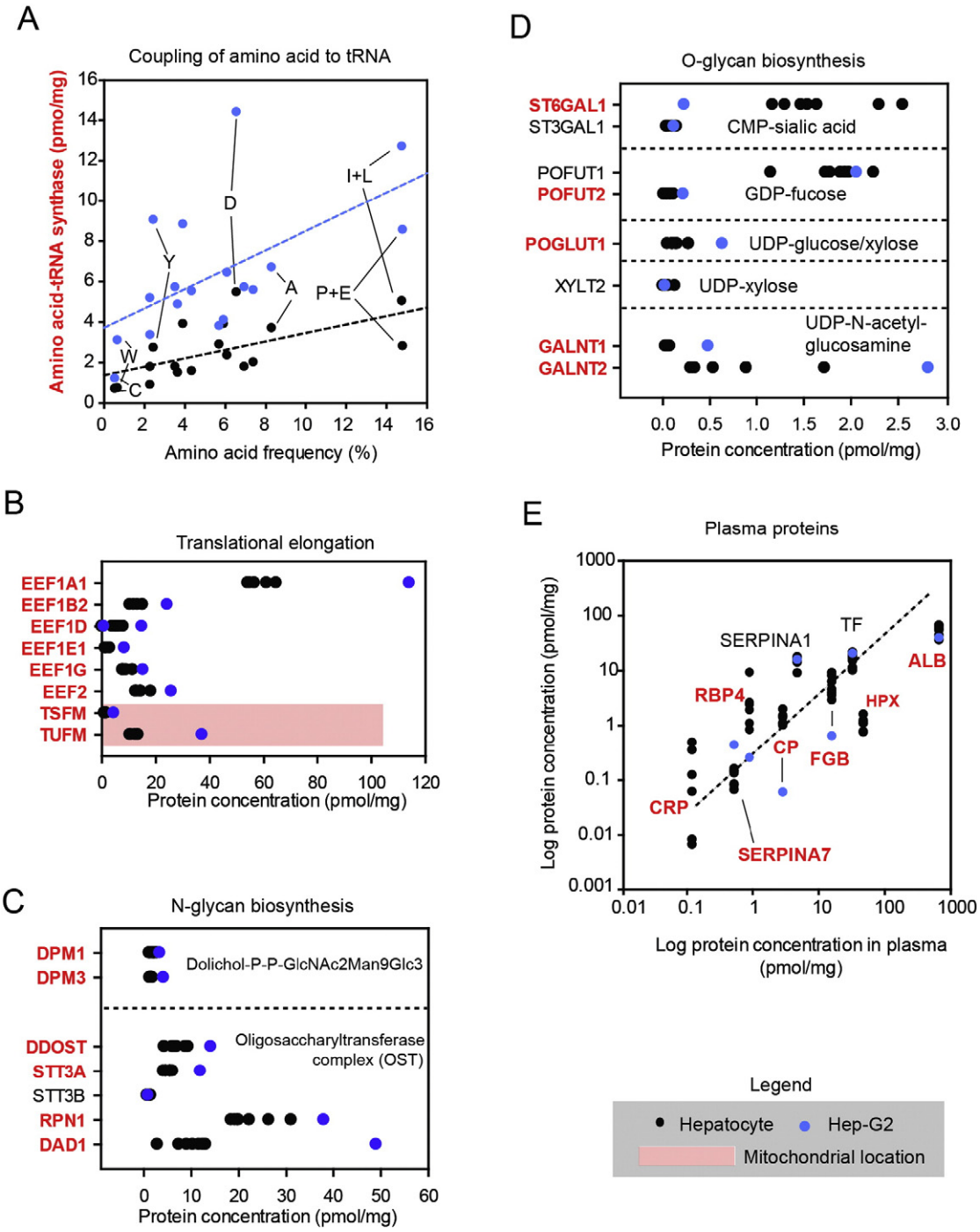

Fig. 5. Concentrations of enzymes involved in various steps of protein synthesis and maturation. (A) Abundance of the amino acid t-RNA ligases as a function of the amino acid frequency observed in the hepatocyte proteome. (B) Concentrations of key proteins involved in polypeptide elongation during translation. (C) Synthesis of dolichol-P-P-GlcNAc$_2$Man$_9$Glc$_3$ for N-glycan synthesis and N-glycan transferases, and (D) O-glycan transferases. (E) Correlation of the abundances of plasma proteins synthesized in hepatocytes and their titers in plasma. Black and blue dots, show average abundance values calculated for the 7 hepatocyte and 3 HepG2 cell samples, respectively. Gene names of proteins ns with statistically significant titer-differences between hepatocyte and HepG2 are in *red* (FDR < 0.05). Arrows indicate statistically significant abundance-differences of the selected protein groups ($P < 0.001$). All amino acid t-RNA ligases showed (A) statistically significant titer-differences (Supplemental Table 3).

HepG2 cells. This may be accompanied with higher needs for NADPH by the mitochondrial cholesterol side chain cleavage system in the hepatocyte mitochondria.

Because NADH produced in the cytoplasm is unable to pass the mitochondrial membranes, it is used by the malate/aspartate shuttle mechanism to regenerate mitochondrial NAD (Fig. 6G). The shuttle involves malate dehydrogenases (*MDH1* and *MDH2*) and aspartate aminotransferases (*GOT1* and *GOT2*) with specific cytoplasmic and mitochondrial locations. Both the cytoplasmic and the mitochondrial enzymes were highly abundant. Another mechanism, known as the glycerol-3-phosphate shuttle, allows regeneration of mitochondrial NAD to NADH using glycerol-3-phosphate, a by-product of glycolysis (Fig. 6F). The mechanism involves cytoplasmic (*GPD1*) and mitochondrial glycerol-3-phosphate dehydrogenase (*GPD2*). The concentrations

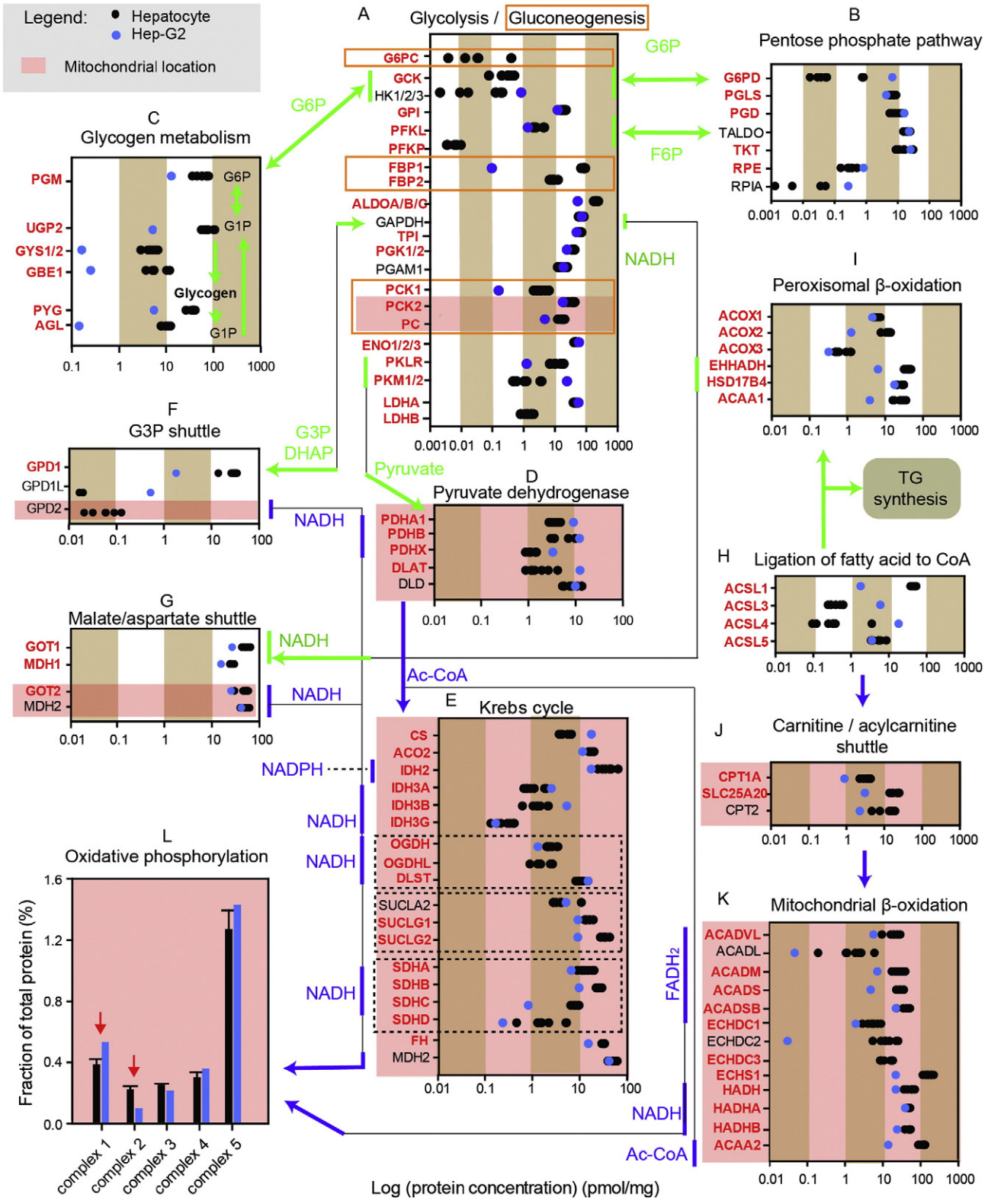

Fig. 6. Energy metabolism. (A) Glycolysis and gluconeogenesis. (B) Pentose phosphate pathway. (C) Glycogen metabolism. (D) Pyruvate dehydrogenase complex. (E) Krebs cycle, (F) Glycerol-3-phosphate shuttle. (G) Malate/aspartate shuttle. (H) Ligation of fatty acids to CoA for lipid synthesis and β-oxidation. (I) Microsomal oxidation of fatty acids. (J) Carnitine/acyl carnitine shuttle (K) Mitochondrial oxidation of fatty acids. (A–K) Protein abundances are expressed in pmol/mg total protein. (L) Summed abundances (total protein) of the complexes involved in oxidative phosphorylation. Black and blue dots, show average abundance values calculated for the 7 hepatocyte and 3 HepG2 cell samples, respectively. Gene names of proteins ns with statistically significant titer-differences between hepatocyte and HepG2 are in red (FDR < 0.05). Arrows in M indicate statistically significant abundance-differences of the selected protein groups ($P < 0.001$).

of these enzymes were lower compared to the enzymes of the malate/aspartate shuttle. This obviously reflects a secondary role of the glycerol-3-phosphate shuttle in the regeneration of mitochondrial NAD.

Ligation to CoA initiates cellular metabolism of free fatty acids. This process is carried out by several ligases. In hepatocytes long-chain-fatty-acid-CoA ligase 1 (*ACSL1*) is the most abundant one, whereas in

HepG2 cells isoform 2 (*ACSL2*) and 3 (*ACSL3*) play the major role (Fig. 6H). In the next step, the CoA-ligated fatty acids can be incorporated into mono-, di- and triglycerides or can be degraded in the process of β-oxidation, which produces Ac-CoA, NADH and $FADH_2$. Palmitic-CoA and shorter aliphatic acid-CoAs are transported into mitochondria by the carnitine/acylacarnitine shuttle for β-oxidation (Fig. 6J and K). Fatty acids with chains longer than 16 carbons are preferentially oxidized in peroxisomes (Fig. 6I). Considering the abundances of key enzymes of β-oxidation, mitochondrial fatty acid oxidation prevails over the same process in peroxisomes. For example, based on the abundances of the last enzyme in the cycle, thiolase (*ACAA1*, *ACCA2*), mitochondria have 5- to 10-fold higher capacity for fatty acid oxidation than peroxisomes. Finally, hepatocytes have about one order of magnitude higher potential to generate energy from fatty acids compared to HepG2 cells.

Beside glycolysis, oxidative phosphorylation is the only cellular process generating ATP in animal cells. For both hepatocytes and HepG2 cells, the sum of all proteins involved in oxidative phosphorylation constituted about 3% of total cellular protein (Fig. 6D). Although the abundances of four complexes of the oxidative phosphorylation cascade were similar for hepatocytes and HepG2 cells, complex II was significantly less abundant in HepG2 cells (Fig. 6L). This may indicate less ATP production via oxidative phosphorylation in the cultured cells and together with the higher titers of hexokinase and the high affinity glucose transporter Glut1 (SLC2A1)(Fig. 7) may reflect the Warburg effect, which is common to cancer cells [35].

3.6. Metabolite transport across plasma membranes

The nutrients and metabolites have to be transferred across cellular membranes by specific transport mechanisms [36]. Our previous work has demonstrated that these membrane proteins can be quantified by our proteomic platform. The present hepatocyte proteome dataset covered about 200 transport proteins, of which 80% belonged to the solute carrier (*SLC*) gene families (Supplemental Table 2). In Fig. 7, a selection of the most prominent transporters of the plasma membrane and mitochondrial outer and inner membranes is shown.

In the plasma membrane of human hepatocytes, the most abundant carrier proteins were the Na^+/K^+ ATPase (*ATP1B*), the passive glucose transporter 2 (GLUT2, *SLC2A2*) and the fatty acid transport protein 2 (FATP2, *SLC27A2*) (Fig. 7A, B, C). They occurred at concentrations of 10 pmol/mg total protein which correspond to on average $2–5 \times 10^6$ copies per cell (Fig. 7E). The plasma membrane also harbors a large number of amino acid transporters, which can be ordered in specific classes according their transport mechanism (Fig. 7D). The cumulative abundance of amino acid transporters in human hepatocyte was on average 1×10^6 copies per cell.

Compared to hepatocytes, the HepG2 cells displayed a quite different composition of transporters in the plasma membrane. The cellular concentrations of the Na^+/K^+-pump and the sarcoplasmic/endoplasmic reticulum calcium ATPase 1 (*ATP2A1*) were 3- and 10-fold higher in HepG2 cells compared to the hepatocytes (Fig. 7A). In HepG2 cells, GLUT2 was replaced by GLUT1 (*SLC2A1*) and GLUT3 (*SLC2A3*) (Fig. 7B). The amino acid transporting systems in the HepG2 cells was differently organized than in the hepatocytes (Fig. 7D). In addition, the cumulative number of the amino acid transporters per cell was higher in HepG2 cells than in hepatocytes (Fig. 7E).

The observed differences of plasma membrane transporters between hepatocytes and HepG2 cells reflect differences in cell metabolism. Whereas β-oxidation of fatty acids dominates in hepatocytes, HepG2 cells preferentially metabolize glucose and amino acids.

3.7. Mitochondrial transport

Generally mitochondria are composed of two layers of membranes, the outer and the inner one. Since membranes are impermeable to metabolites, the latter are transported across the membranes by pumps and shuttle mechanisms. To obtain precise insights into the organization of mitochondrial transport we expressed concentrations per mitochondrial fraction (Fig. 7F–L) and protein copy numbers of mitochondrial transporters per single mitochondrion (Fig. 7M). To calculate the mitochondrial concentrations we used the values of total mitochondrial protein contents of 25% and 12% in hepatocytes and HepG2 cells, respectively (Fig. 2B). For calculation of the protein copies per mitochondrion we assumed 2000 mitochondria per hepatocyte [37] and 250 mitochondria per HepG2 cell. The latter value is an average number of mitochondria observed in cultured cells [38].

The metabolite transport via the outer mitochondrial membrane is regulated by voltage-dependent anion channel (VDAC) proteins that are also known as porins. In hepatocytes and HepG2 cells we identified three isoforms of VDACs (Fig. 7F). VDAC1 was the most abundant in both cell types. However, the concentration of VDAC1 in the hepatocyte mitochondria was about one order of magnitude lower than in the mitochondria of HepG2. Similar differences were also observed for the VDAC2 and VDAC3 isoforms. Thus, our data most probably indicate large differences in the organization of the outer mitochondrial membrane. On the other hand, the higher abundance of the VDACs in HepG2 can also be partially attributed to the occurrence of porins in plasma membranes [39].

The inner mitochondrial membrane harbors a large number of transport proteins. The most abundant ones were the ADP/ATP translocases (*SLC25A4*, *5* and 6) and the phosphate pump (*SLC25A3*), which are the key components of the ATP synthase machinery (Fig. 7G). Transporters involved in metabolite shuttling constitute the next group of abundant proteins located in the inner membrane (Fig. 7H, I, J, K, and L). In contrast to porins, the concentrations of many of these transporters were comparable in hepatocytes and HepG2 cells with some exceptions. For example, the citrate/malate and dicarboxylate transporters (Fig. 7H) were more abundant in HepG2 cells than hepatocytes. These differences correlate well with higher citrate synthase titers in HepG2 cells (Fig. 6E). Moreover, the acylcarnitine/carnitine transporter (Fig. 7K) occurred at significantly higher concentration in hepatocytes compared to HepG2 cells reflecting high fatty acid catabolism in hepatocytes (Fig. 6J and K).

Finally, expressing the protein abundances in copy numbers, we calculated that a single mitochondrion in the hepatocyte contains 5000–10,000 porins and ATP translocases (Fig. 6M). The pyruvate and the carnitine transporters were 2–3 times less abundant than the porins and ATP translocases. The ornithine transporter occurred in 1000 copies on average, whereas transport of CoA is carried out by only 100–500 molecules. The mitochondria of HepG2 cells differed from that of hepatocytes by higher abundances of the porins and lower copy numbers for ornithine, carnitine, and CoA transporters.

3.8. Uptake, metabolism, and efflux of drugs

Hepatocytes play an important role in the elimination of drugs and other xenobiotic compounds from the blood circulation. The hepatobiliary elimination consists of the following phases: basolateral uptake (Fig. 8A), phase I and phase II metabolism (Fig. 8B and C), and biliary/sinusoidal efflux (Fig. 8D). In general, membrane transport proteins of the solute carrier (*SLC*) family facilitate the hepatic uptake of drugs, while excretion into the bile and blood is carried out by transporters of the ATP-binding cassette (*ABC*) family. By determining the amount of drug that enters and exits the cell, the transport proteins may also influence the rate and extent of drug metabolism.

Analysis of the whole cell lysates revealed that the most abundant uptake transporters in the basolateral membrane of the hepatocytes were organic anion transporting polypeptide 1B1 (OATP1B1, *SLCO1B1*), OATP1B3 (*SLCO1B3*), and organic cation transporter 1 (OCT1, *SLC22A1*). They occurred at concentrations of around 1 pmol/mg total protein which corresponds to on average $4–7 \times 10^5$ copies per cell. The sodium-taurocholate transporting polypeptide (NTCP, *SLC10A1*), which

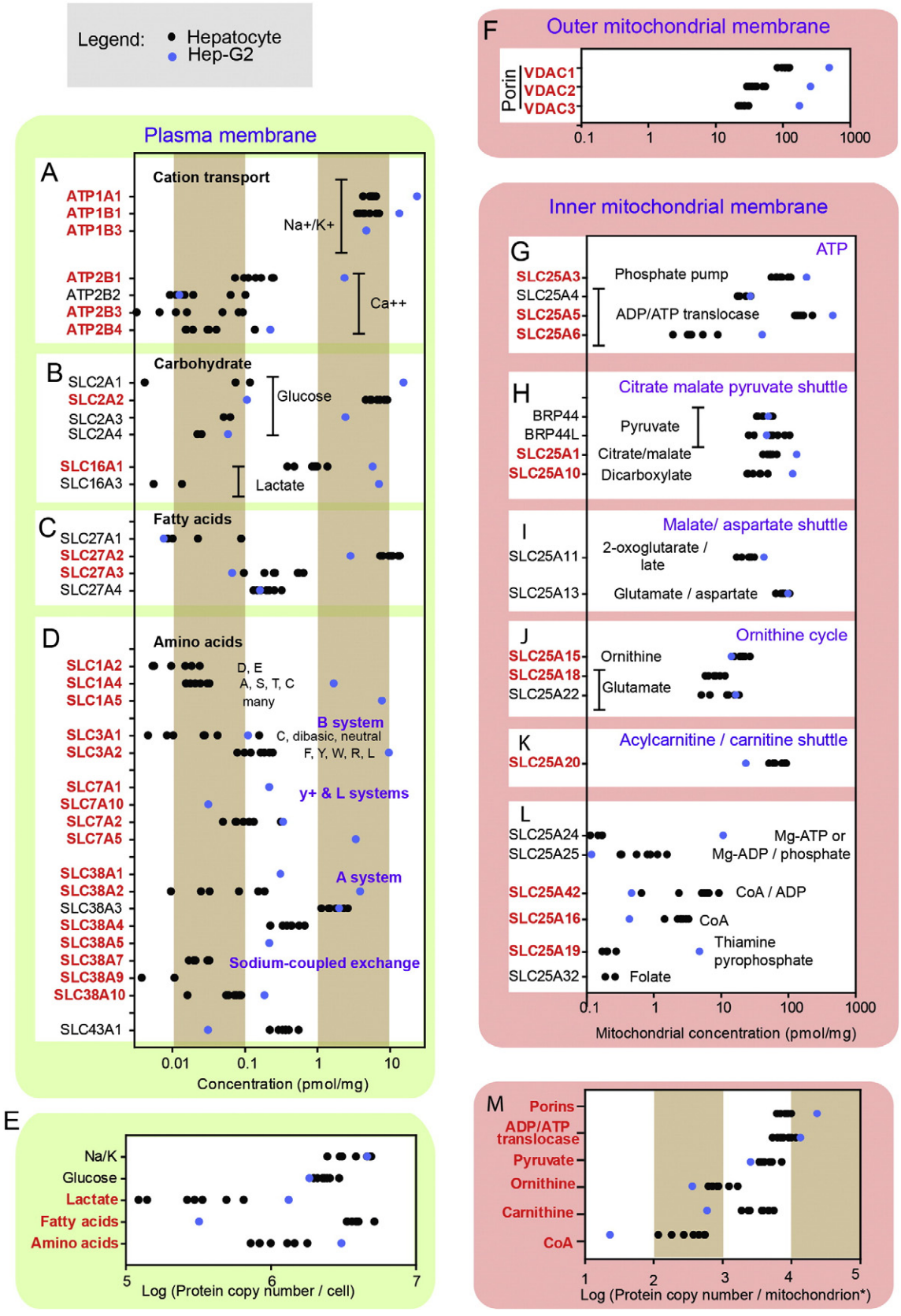

Fig. 7. Abundances of nutrient and metabolite transport across the plasma (A–E) and mitochondrial membranes (F–J). (A–D) Concentrations of plasma membrane transporters for cations (A); glucose and lactate (B); fatty acids (C), and amino acids. In D, the amino acid specificity of some transporters is indicated using the single amino acid code. (E) Protein copy numbers of selected transporters. Concentrations of porin subunits in the outer mitochondrial membrane (F) and transporters in the inner mitochondrial membrane (G-L). (M) Protein copy numbers per mitochondrion of selected transporters. The values were calculated under the assumption of 2000 mitochondria per hepatocyte and 250 mitochondria per HepG2 cell, respectively. Black and blue dots, show average abundance values calculated for the 7 hepatocyte and 3 HepG2 cell samples, respectively. Gene names of proteins ns with statistically significant titer-differences between hepatocyte and HepG2 are in red (FDR < 0.05). Arrows indicate statistically significant abundance-differences of the selected protein groups ($P < 0.001$).

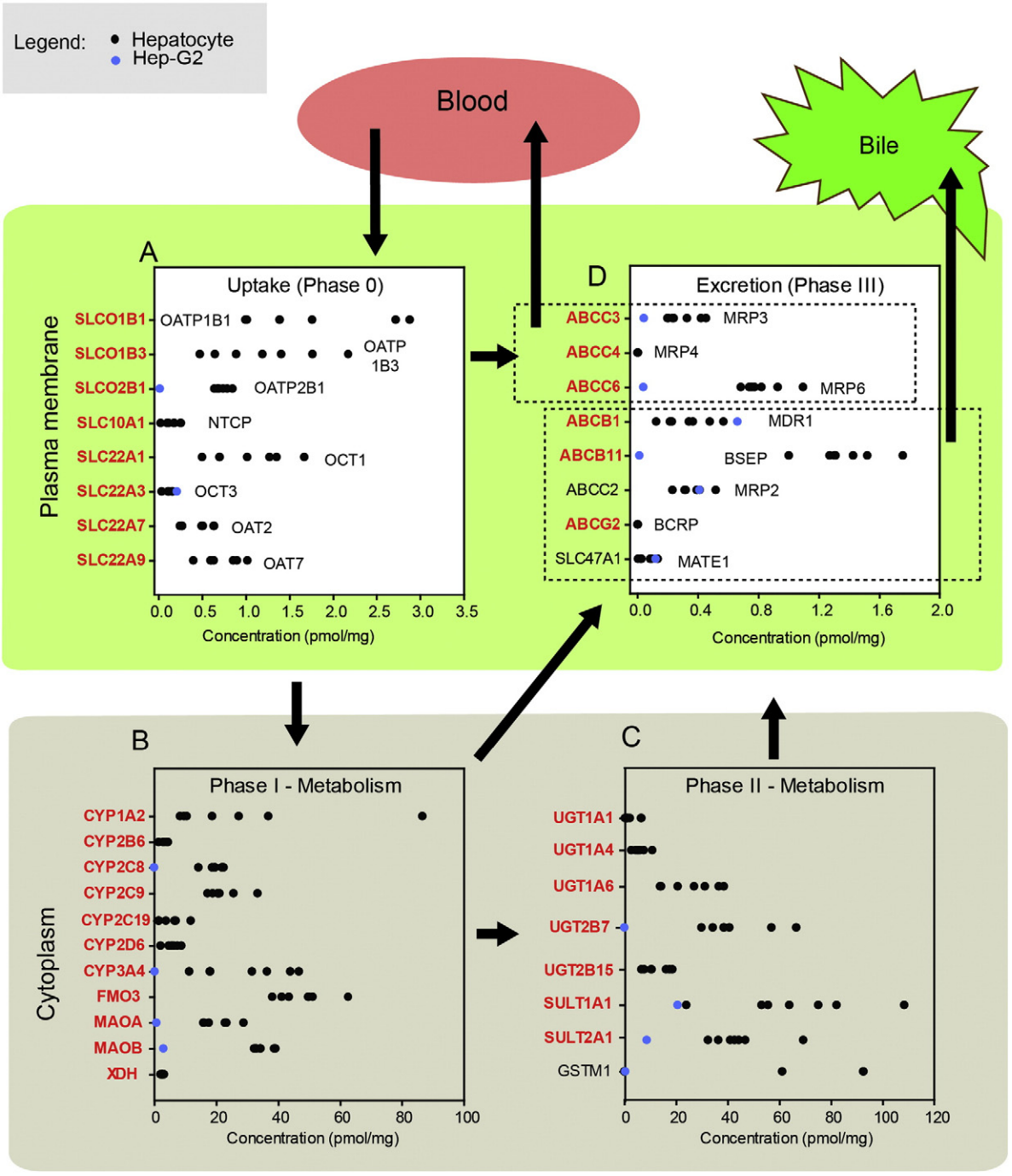

Fig. 8. Abundances of key proteins for drug transport and metabolism. (A) Uptake transporters in the basolateral membrane. (B) Enzymes of drug oxidation (phase I metabolism). (C) Enzymes of phase II drug metabolism. (D) Efflux transporters in the canalicular and basolateral membrane. Black and blue dots show average abundance values calculated for the 7 hepatocyte and 3 HepG2 cell samples, respectively. Gene names of proteins with statistically significant titer-differences for hepatocytes and HepG2 cells are in red (FDR < 0.05).

is the major hepatic uptake transporter of bile acids from the blood, was about one order of magnitude less abundant. In contrast to hepatocytes, the HepG2 cells failed to display OATP1B1, OATP1B3, OCT1, and NTCP in quantifiable levels.

Phase I metabolizing enzymes introduce reactive or polar groups into their substrates and were expressed in the hepatocytes in levels comparable to those reported for human liver tissue [13,40]. In the HepG2 cells, these enzymes were either absent or expressed in very low amounts (Fig. 8B). This included the important CYP3A4 enzyme, which was 100- to 400-fold more abundant in the hepatocytes than in the HepG2 cells. Other significant drug-metabolizing CYP enzymes, such as CYP1A2, CYP2B6, CYP2C9, CYP2C19, and CYP2D6, displayed concentrations of 3–28 pmol/mg total protein on average in the hepatocytes, whereas the levels were not quantifiable in the HepG2 cells. Interestingly, the related cell line HepaRG expresses some of these enzymes [41]. Their protein concentrations in HepaRG cells are, however, unknown.

Contrary to the phase I enzymes, the phase II enzymes, which form conjugates with charged molecules such as sulfate, glucuronic acid and glutathione, differed to a variable extent between the hepatocytes and the HepG2 cells. While SULT1A1, SULT2A1 were expressed at almost similar titers in the hepatocytes and HepG2 cells, the expression

of other phase II enzymes, including UGT1A1, UGT1A4, UGT1A6, UGT2B7, UGT2B15, and GSTM1, was not present or very low in the HepG2 cells compared to the hepatocytes.

Conjugates from phase II metabolism are excreted into the bile and/or the blood by efflux transporters in the canalicular and basolateral membrane of the hepatocytes, respectively. This process is sometimes referred to as phase III metabolism. The most abundant efflux transporter in the canalicular membrane of the hepatocytes was the bile salt export pump (BSEP, *ABCB11*) at 1.4 pmol/mg total protein, followed by multidrug resistance-associated protein 2 (MRP2, *ABCC2*) and multidrug resistance protein 1 (MDR1, *ABCB1*). Most of the canalicular efflux transporters were present in the HepG2 cells at levels close to those found in hepatocytes. BSEP titers were, however, 100-fold lower in the HepG2 cells than in the hepatocytes. These findings are supported by studies on mRNA level [42,43]. The titers of the basolateral efflux transporters MRP3 and MRP6 were 4- to 20-fold lower in the HepG2 cells than in hepatocytes, whereas MRP4 was not present in the HepG2 cells.

In summary, the shortage of uptake transporters and phase I enzymes clearly limits the use of HepG2 cells for the prediction of xenobiotic metabolism and elimination. Our findings are in agreement with previous studies at the mRNA [43–45] and protein levels [13,40].

4. Conclusions

Technological progress in proteomics offers quantitative analysis of tissues and cells encompassing the entire proteome. Notably, it is now possible to do such analyses without laborious preparation of standards or generation of calibration curves. Protein titers and copy numbers can be assessed directly from proteomic data using the TPA and 'Proteomic Ruler' methods. We applied these computational advancements to study the human hepatocyte proteome. We draw a virtual picture of this cell providing information of its size, subcellular composition and abundance of specific proteins, protein complexes, and pathways. Notably, we provide the first in-depth comparative and quantitative proteomic analysis of human adult hepatocytes and HepG2 cells. The dataset can be used to match the titer data with biochemically assessed enzyme and/or transporter kinetic parameters for systems biology modeling approaches [11,25].

Our data delineate extensive differences between human hepatocytes and cultured HepG2 cells. These are in line with previously published results comparing relative protein levels of 432 proteins between cultured human adult hepatocytes and the HepG2 cells [46]. In contrast to that work our data quantitatively describe protein titers and demonstrate alterations between the freshly isolated hepatocytes and cultured cells. The huge differences in the titers of drug uptake and excretion transporters and Phase I and II metabolism enzymes questions the value of HepG2 cells as an in vitro model for pharmaco- and toxicokinetic studies.

Supplementary data to this article can be found online at http://dx.doi.org/10.1016/j.jprot.2016.01.016.

Conflict of interest

The authors declare no competing financial interest.

Acknowledgements

We thank Prof. Matthias Mann (Max-Planck Institute, Martinsried) for continuous support, Katharina Zettl for technical assistance and Igor Paron and Korbinian Mayr for support in mass spectrometric analysis. Prof. Dariusz Rakus (Wroclaw University) is acknowledged for critical reading of the manuscript. This work was supported by the Max-Planck Society for the Advancement of Science and the Swedish Research Council (grant no 2822).

References

[1] H. Lodish, A. Berk, S. Zipursky, P. Matsudaira, D. Baltimore, J. Darnell, Molecular Cell Biology, fourth ed. W.H. Freeman, New York, 2000.
[2] E.R. Weibel, W. Staubli, H.R. Gnagi, F.A. Hess, Correlated morphometric and biochemical studies on the liver cell. I. Morphometric model, stereologic methods, and normal morphometric data for rat liver, J. Cell Biol. 42 (1969) 68–91.
[3] M.N. Berry, Edwards AM, The Hepatocyte Review, Kulwer Academic Publishers, 2000.
[4] P. Godoy, N.J. Hewitt, U. Albrecht, M.E. Andersen, N. Ansari, S. Bhattacharya, et al., Recent advances in 2D and 3D in vitro systems using primary hepatocytes, alternative hepatocyte sources and non-parenchymal liver cells and their use in investigating mechanisms of hepatotoxicity, cell signaling and ADME, Arch. Toxicol. 87 (2013) 1315–1530.
[5] E. Ramboer, T. Vanhaecke, V. Rogiers, M. Vinken, Immortalized human hepatic cell lines for in vitro testing and research purposes, Methods Mol. Biol. 1250 (2015) 53–76.
[6] E. Berger, N. Vega, M. Weiss-Gayet, A. Geloen, Gene network analysis of glucose linked signaling pathways and their role in human hepatocellular carcinoma cell growth and survival in HuH7 and HepG2 cell lines, Biomed. Res. Int. 2015 (2015) 821761.
[7] J.R. Wisniewski, K. Dus, M. Mann, Proteomic workflow for analysis of archival formalin-fixed and paraffin-embedded clinical samples to a depth of 10 000 proteins, Proteomics Clin. Appl. 7 (2013) 225–233.
[8] J.R. Wisniewski, P. Ostasiewicz, M. Mann, High recovery FASP applied to the proteomic analysis of microdissected formalin fixed paraffin embedded cancer tissues retrieves known colon cancer markers, J. Proteome Res. 10 (2011) 3040–3049.
[9] J.R. Wisniewski, P. Ostasiewicz, K. Dus, D.F. Zielinska, F. Gnad, M. Mann, Extensive quantitative remodeling of the proteome between normal colon tissue and adenocarcinoma, Mol. Syst. Biol. 8 (2012) 611.
[10] J.R. Wisniewski, M.Y. Hein, J. Cox, M. Mann, A "proteomic ruler" for protein copy number and concentration estimation without spike-in standards, Mol. Cell. Proteomics 13 (2014) 3497–3506.
[11] A. Vildhede, M. Karlgren, E.K. Svedberg, J.R. Wisniewski, Y. Lai, A. Noren, et al., Hepatic uptake of atorvastatin: influence of variability in transporter expression on uptake clearance and drug–drug interactions, Drug Metab. Dispos. 42 (2014) 1210–1218.
[12] M. Karlgren, A. Vildhede, U. Norinder, J.R. Wisniewski, E. Kimoto, Y. Lai, et al., Classification of inhibitors of hepatic organic anion transporting polypeptides (OATPs): influence of protein expression on drug–drug interactions, J. Med. Chem. 55 (2012) 4740–4763.
[13] A. Vildhede, J.R. Wisniewski, A. Noren, M. Karlgren, P. Artursson, Comparative proteomic analysis of human liver tissue and isolated hepatocytes with a focus on proteins determining drug exposure, J. Proteome Res. 14 (2015) 3305–3314.
[14] J.R. Wisniewski, A. Friedrich, T. Keller, M. Mann, H. Koepsell, The impact of high fat diet on metabolism and immune defense in small intestine mucosa, J. Proteome Res. (2014).
[15] J.R. Wisniewski, H. Koepsell, A. Gizak, Rakus D., Absolute protein quantification allows differentiation of cell specific metabolic routes and functions, Proteomics (2014).
[16] D. Rakus, A. Gizak, A. Deshmukh, Wisniewski JR, Absolute quantitative profiling of the key metabolic pathways in slow and fast skeletal muscle, J. Proteome Res. (2015).
[17] E.L. Lecluyse, E. Alexandre, Isolation and culture of primary hepatocytes from resected human liver tissue, Methods Mol. Biol. 640 (2010) 57–82.
[18] P.A. Nielsen, J.V. Olsen, A.V. Podtelejnikov, J.R. Andersen, M. Mann, J.R. Wisniewski, Proteomic mapping of brain plasma membrane proteins, Mol. Cell. Proteomics 4 (2005) 402–408.
[19] J.R. Wisniewski, M. Mann, Consecutive proteolytic digestion in an enzyme reactor increases depth of proteomic and phosphoproteomic analysis, Anal. Chem. 84 (2012) 2631–2637.
[20] J.R. Wisniewski, F.Z. Gaugaz, Fast and sensitive total protein and peptide assays for proteomic analysis, Anal. Chem. 87 (2015) 4110–4116.
[21] J.R. Wisniewski, A. Zougman, M. Mann, Combination of FASP and StageTip-based fractionation allows in-depth analysis of the hippocampal membrane proteome, J. Proteome Res. 8 (2009) 5674–5678.
[22] J.R. Wisniewski, G. Prus, Homogenous phase enrichment of cysteine-containing peptides for improved proteome coverage, Anal. Chem. 87 (2015) 6861–6867.
[23] J.R. Wisniewski, D. Rakus, Multi-enzyme digestion FASP and the 'Total Protein Approach'-based absolute quantification of the *Escherichia coli* proteome, J. Proteome 109 (2014) 322–331.
[24] B.R. Dimayacyac-Esleta, C.F. Tsai, R.B. Kitata, Lin PY, Choong WK, Lin TD, et al., Rapid high-pH reverse phase StageTip for sensitive small-scale membrane proteomic profiling, Anal. Chem. (2015).
[25] P. Matsson, L.A. Fenu, P. Lundquist, J.R. Wisniewski, M. Kansy, P. Artursson, Quantifying the impact of transporters on cellular drug permeability, Trends Pharmacol. Sci. 36 (2015) 255–262.
[26] D. Rakus, A. Gizak, A. Deshmukh, J.R. Wisniewski, Absolute quantitative profiling of the key metabolic pathways in slow and fast skeletal muscle, J. Proteome Res. 14 (2015) 1400–1411.
[27] J.R. Wisniewski, K. Dus-Szachniewicz, P. Ostasiewicz, P. Ziolkowski, D. Rakus, M. Mann, Absolute proteome analysis of colorectal mucosa, adenoma, and cancer reveals drastic changes in fatty acid metabolism and plasma membrane transporters, J. Proteome Res. 14 (2015) 4005–4018.
[28] D.L. Schmucker, Aging and the liver: an update, J. Gerontol. A Biol. Sci. Med. Sci. 53 (1998) B315–B320.

[29] H. Toyoda, O. Bregerie, A. Vallet, B. Nalpas, G. Pivert, C. Brechot, et al., Changes to hepatocyte ploidy and binuclearity profiles during human chronic viral hepatitis, Gut 54 (2005) 297–302.
[30] T. Watanabe, Y. Tanaka, Age-related alterations in the size of human hepatocytes. A study of mononuclear and binucleate cells, Virchows Arch. B. 39 (1982) 9–20.
[31] G.C. Brown, Total cell protein concentration as an evolutionary constraint on the metabolic control distribution in cells, J. Theor. Biol. 153 (1991) 195–203.
[32] I. Brockhausen, H. Schachter, P. Stanley, O-GalNAc Glycans, in: A. Varki, Cummings RD, Esko JD, Freeze HH, P. Stanley, Bertozzi CR, et al., (Eds.), Essentials of Glycobiology, second ed.Cold Spring Harbor, NY, 2009.
[33] P. Stanley, H. Schachter, N. Taniguchi, N-Glycans, in: A. Varki, Cummings RD, Esko JD, Freeze HH, P. Stanley, Bertozzi CR, et al., (Eds.), Essentials of Glycobiology, second ed.Cold Spring Harbor, NY, 2009.
[34] A. Varki, R. Schauer, Sialic Acids, in: A. Varki, Cummings RD, Esko JD, Freeze HH, P. Stanley, Bertozzi CR, et al. (Eds.), Essentials of Glycobiology, second ed.Cold Spring Harbor, NY, 2009.
[35] M.G. Vander Heiden, L.C. Cantley, C.B. Thompson, Understanding the Warburg effect: the metabolic requirements of cell proliferation, Science 324 (2009) 1029–1033.
[36] International Transporter C, K.M. Giacomini, S.M. Huang, D.J. Tweedie, L.Z. Benet, K.L. Brouwer, et al., Membrane transporters in drug development, Nat. Rev. Drug Discov. 9 (2010) 215–236.
[37] B. Alberts, A. Johnson, J. Lewis, M. Raff, K. Roberts, P. Walter, Molecular Biology of the Cell, Garland Publishing Inc., New York, 1994.
[38] E.D. Robin, R. Wong, Mitochondrial DNA molecules and virtual number of mitochondria per cell in mammalian cells, J. Cell. Physiol. 136 (1988) 507–513.
[39] V. De Pinto, A. Messina, D.J. Lane, A. Lawen, Voltage-dependent anion-selective channel (VDAC) in the plasma membrane, FEBS Lett. 584 (2010) 1793–1799.
[40] B. Achour, J. Barber, A. Rostami-Hodjegan, Expression of hepatic drug-metabolizing cytochrome p450 enzymes and their intercorrelations: a meta-analysis, Drug Metab. Dispos. 42 (2014) 1349–1356.
[41] A. Guillouzo, A. Corlu, C. Aninat, D. Glaise, F. Morel, C. Guguen-Guillouzo, The human hepatoma HepaRG cells: a highly differentiated model for studies of liver metabolism and toxicity of xenobiotics, Chem. Biol. Interact. 168 (2007) 66–73.
[42] M. Le Vee, E. Jigorel, D. Glaise, P. Gripon, C. Guguen-Guillouzo, O. Fardel, Functional expression of sinusoidal and canalicular hepatic drug transporters in the differentiated human hepatoma HepaRG cell line, Eur. J. Pharm. Sci. 28 (2006) 109–117.
[43] T.K. Lee, C.L. Hammond, N. Ballatori, Intracellular glutathione regulates taurocholate transport in HepG2 cells, Toxicol. Appl. Pharmacol. 174 (2001) 207–215.
[44] W.M. Westerink, W.G. Schoonen, Cytochrome P450 enzyme levels in HepG2 cells and cryopreserved primary human hepatocytes and their induction in HepG2 cells, Toxicol. in Vitro 21 (2007) 1581–1591.
[45] S. Wilkening, F. Stahl, A. Bader, Comparison of primary human hepatocytes and hepatoma cell line Hepg2 with regard to their biotransformation properties, Drug Metab. Dispos. 31 (2003) 1035–1042.
[46] C. Rowe, D.T. Gerrard, R. Jenkins, A. Berry, K. Durkin, L. Sundstrom, et al., Proteome-wide analyses of human hepatocytes during differentiation and dedifferentiation, Hepatology 58 (2013) 799–809.
[47] J.A. Vizcaino, E.W. Deutsch, R. Wang, A. Csordas, F. Reisinger, D. Rios, et al., ProteomeXchange provides globally coordinated proteomics data submission and dissemination, Nat. Biotechnol. 32 (2014) 223–226.